New Diagnostic Capabilities for NASA's Pulsed Nanosecond Discharge

B. T. Yee, J. E. Foster

University of Michigan, Ann Arbor, MI 48109

S. J. Schneider, I. M. Blankson

NASA Glenn Research Center, Cleveland, OH 44135

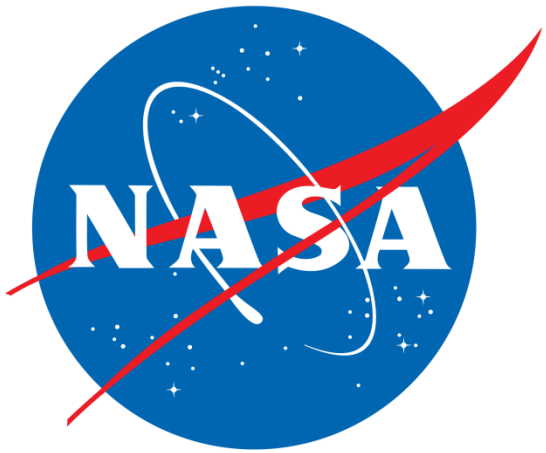

MICHIGAN

I. Motivation

1. Plasmas are attractive in material processing, hypersonics and other applications, leading to a demand for large volume, high pressure, uniform sources. Pulsed nanosecond discharges fill these requirements.
2. The evolution of physical parameters in pulsed nanosecond discharges is not well known and the discharge mechanisms are poorly understood.
3. Measurements of parameters provides important validation of modeling efforts and insight on the plasma chemistry and excitation processes.
4. Interferometry gives electron density, optical emission spectroscopy (OES) the system temperatures and coherent anti-Stokes Raman scattering (CARS) spectroscopy may yield electric field information[1].

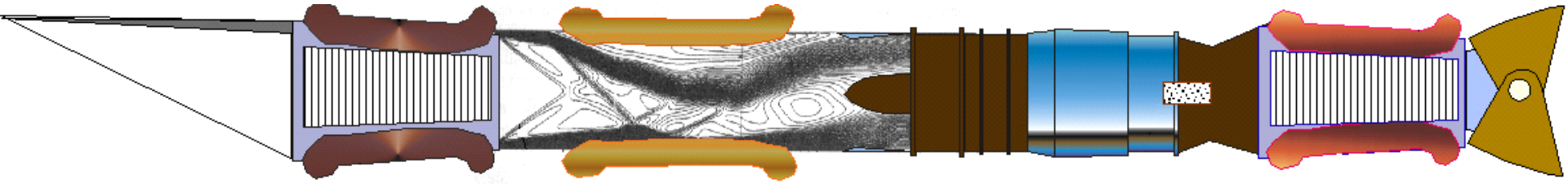

Fig. 1 Hypersonic turbojet engine enabled by MHD bypass and pulsed nanosecond discharge. [2]

II. Physical Principle of the Ionization Wave Discharge

- Discharge depends on large dV/dt (> 10 kV/ns)
- Electrons are accelerated to run-away regime without streamer formation
- Ionization "wave" crosses from cathode to anode
  - Dominant ionization mechanisms: collisional and photo
- Yields large volume ionization of near atmospheric gases

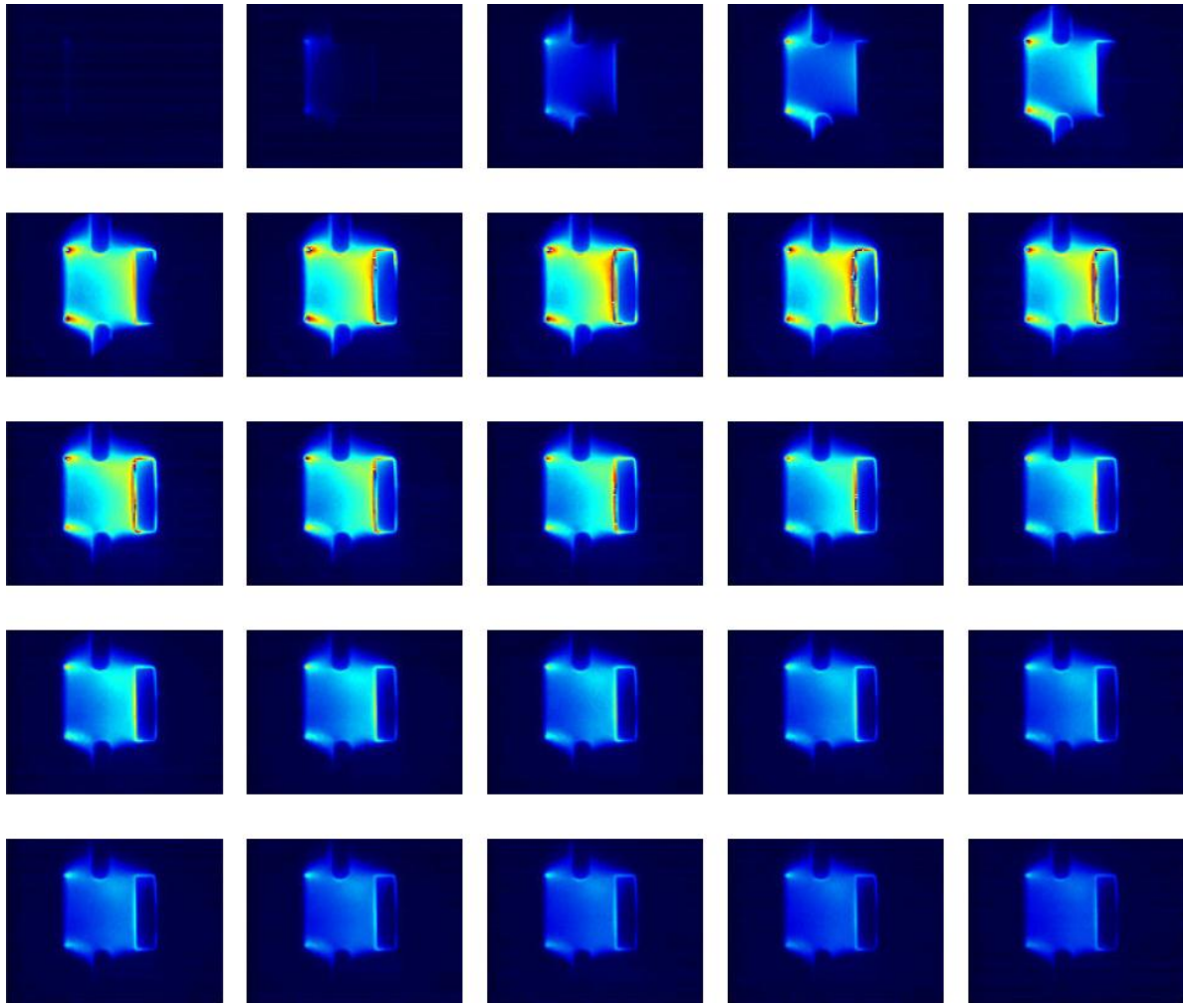

Fig. 2 ICCD images of the evolution of a pulsed nanosecond discharge in 1 ns intervals. The discharge was operated at 40 kHz in 50 Torr of dry air. [1]

IIIa. Simulations (Model)

- Predicts electron density, sheath boundary, and electric fields based on approximations made by Nikandrov et al. [3]

- Electric field spatial profile approximated as an offset Heaviside function

- Electron density in sheath is taken to be zero and an initial density of 10^7 cm^{-3} is assumed

- Diffusion effects neglected; ionization wave time scale is much shorter than diffusion time scale

IIIb. Simulations (Model)

- Quasi-analytic solution of drift equations possible
- Iterative solution required for electric field in bulk plasma
- Test case in Nikandrov used to verify code

$$\frac{dn_e}{dt} = -\alpha \mu_e n_e E$$

$$e\mu_e E_{pl} n_e + \varepsilon_0 \frac{d}{dt}\left(E_{pl} - E_{sh}\right) = 0$$

$$E_{pl}\left(L - X\right) + E_{sh}\left(\frac{2d}{\varepsilon} + X\right) = U(t)$$

IIIc. Simulations (Results)

- Electric field in sheath and plasma deviate from vacuum field as sheath relaxes
- Peak electron density agrees well with Schneider et al. [3]
- Sheath undergoes expands with the voltage pulse and relaxes on a time scale of 30ns
- Electron density quickly reaches plateau, no loss terms included in model

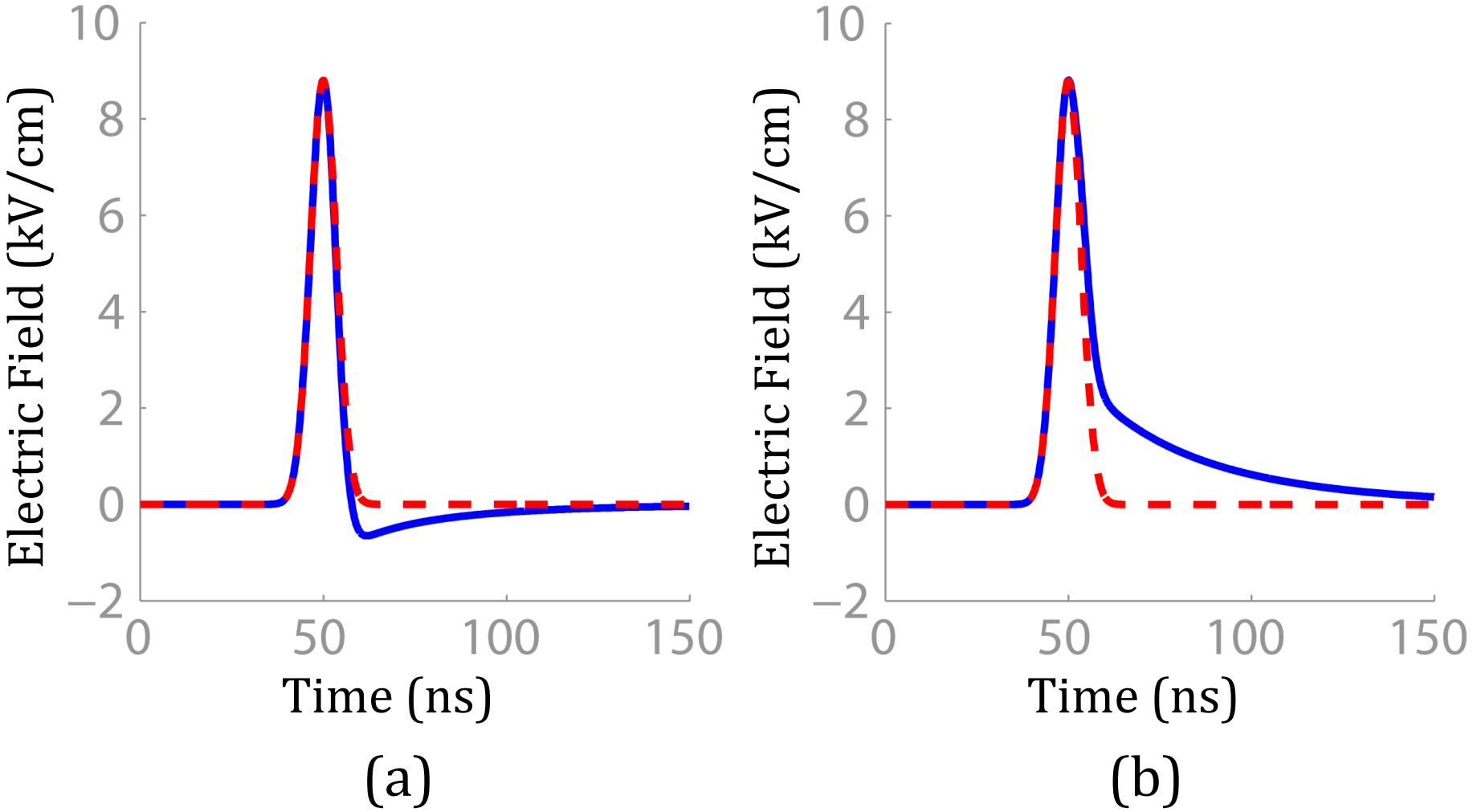

Fig. 4 Red dotted lines represent the vacuum field values.
(a) Electric field values within the bulk of the plasma.
(b) Electric field values within the sheath.

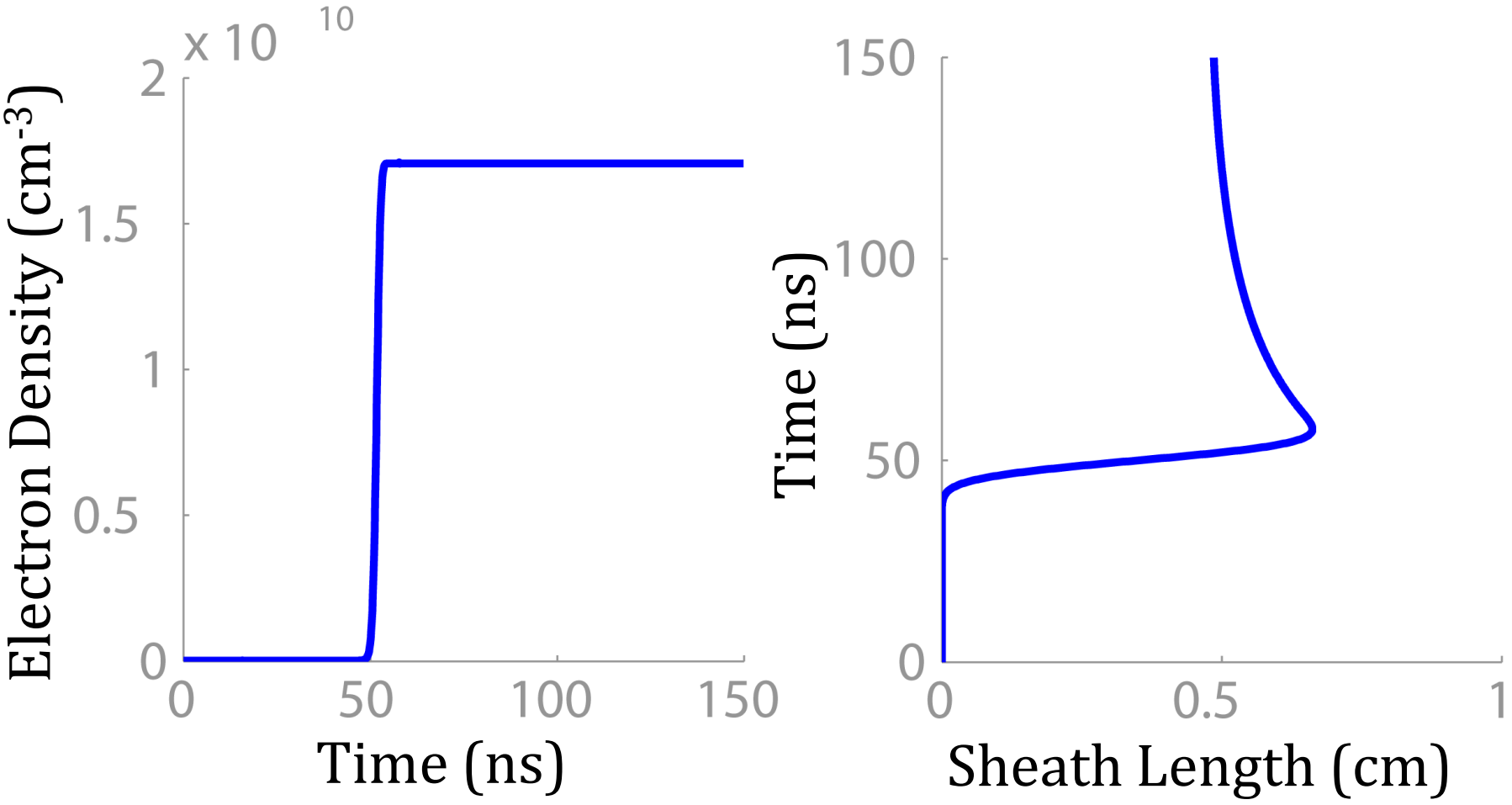

Fig. 5 Modeling of the time evolution of the electron density as well as the movement of the sheath boundary in a pulsed nanosecond discharge.

IVa. Experimental Description (Discharge)

- ~1 cubic foot vacuum facility, dry scroll pumped
- Backfilled with dry air to operating pressure (10-80 Torr)
- Pulsed nanosecond discharge power supply (6-100 kHz, ≤60 kV, FWHM 5 ns)
  - Circular, planar electrodes, 2.5 cm in diameter, adjustable spacing
- Floating sustainer power supply (≤ 1kV)
  - Cylindrical electrodes, 0.6 cm in diameter
  - Sustains charged particle population between pulses

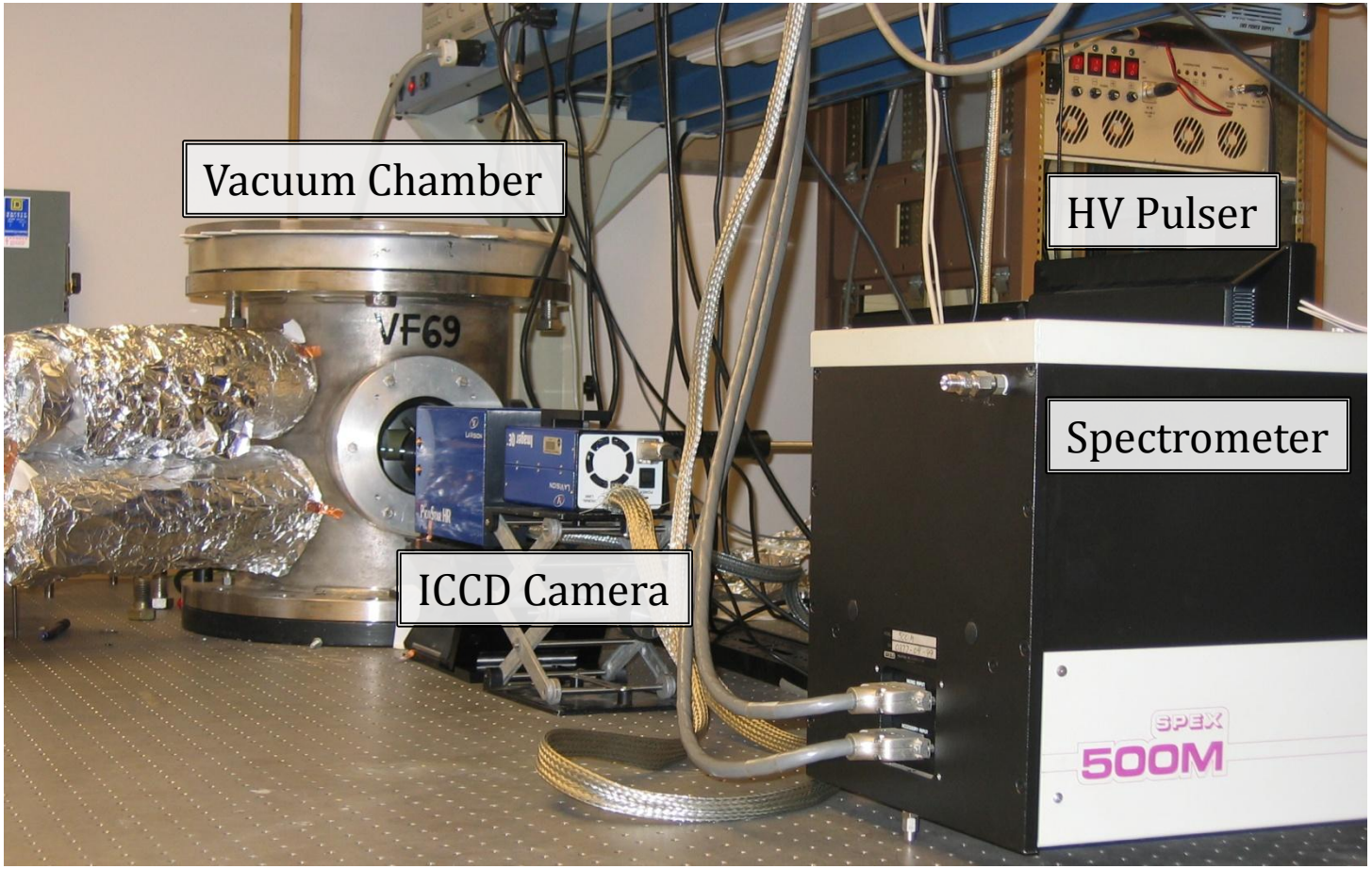

Fig. 6 Photograph of the experimental facilities located at NASA Glenn Research Center

V. Optical Emission Spectroscopy

- Data obtained by fiber coupled Spex 500M with photomultiplier tube
  - 1800 grooves/mm grating
  - 50 μm slit widths

- Preliminary measurements made of first negative nitrogen bands

- Plans to change to ICCD detector for time-resolved measurements

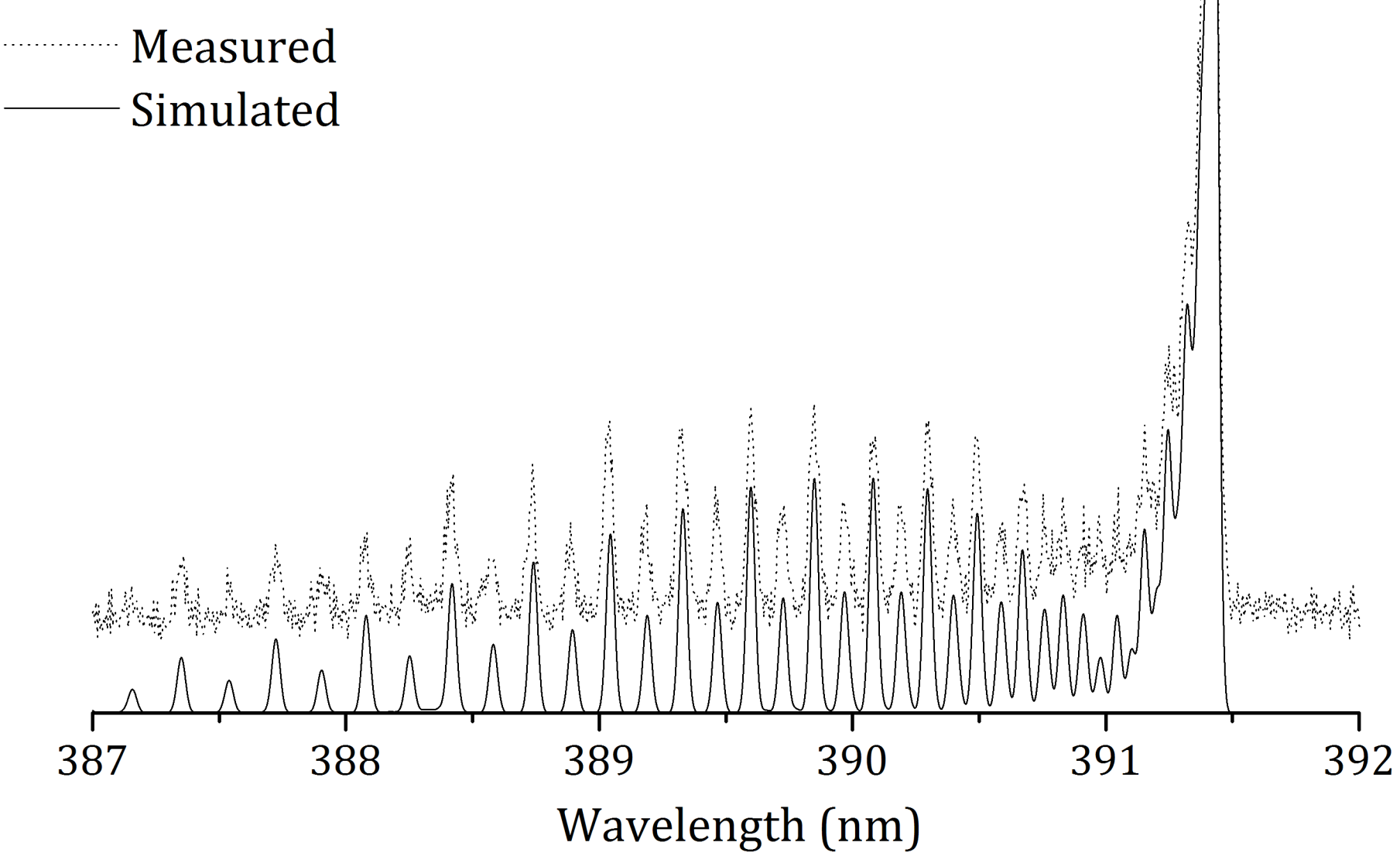

Fig. 7 Comparison of the measured first negative nitrogen spectrum, $B^2\Sigma_u^+ \rightarrow X^2\Sigma_g^+$, to one simulated by Specair[4] with a rotational temperature of 900 K.

VI. mm-Wave Interferometry

- Transmission coefficients measured with Hewlett-Packard 8510C vector network analyzer
  - W-band (75-110 GHz) test set

- Free charge in plasma and collisions lead to a complex index of refraction expressed by Appleton-Hartree equations,

$$\beta_p, \alpha_p = \frac{\omega}{c}\left\{ \pm \frac{1}{2}\left(1 - \frac{\omega_p^2}{\omega^2 + \nu_{eff}^2}\right) + \frac{1}{2}\left[\left(1 - \frac{\omega_p^2}{\omega^2 + \nu_{eff}^2}\right)^2 + \left(\frac{\omega_p^2}{\omega^2 + \nu_{eff}^2}\frac{\nu_{eff}}{\omega}\right)^2\right]^{1/2}\right\}^{1/2}$$

- Measured phase shift and amplitude change data used to produce density and collision frequency

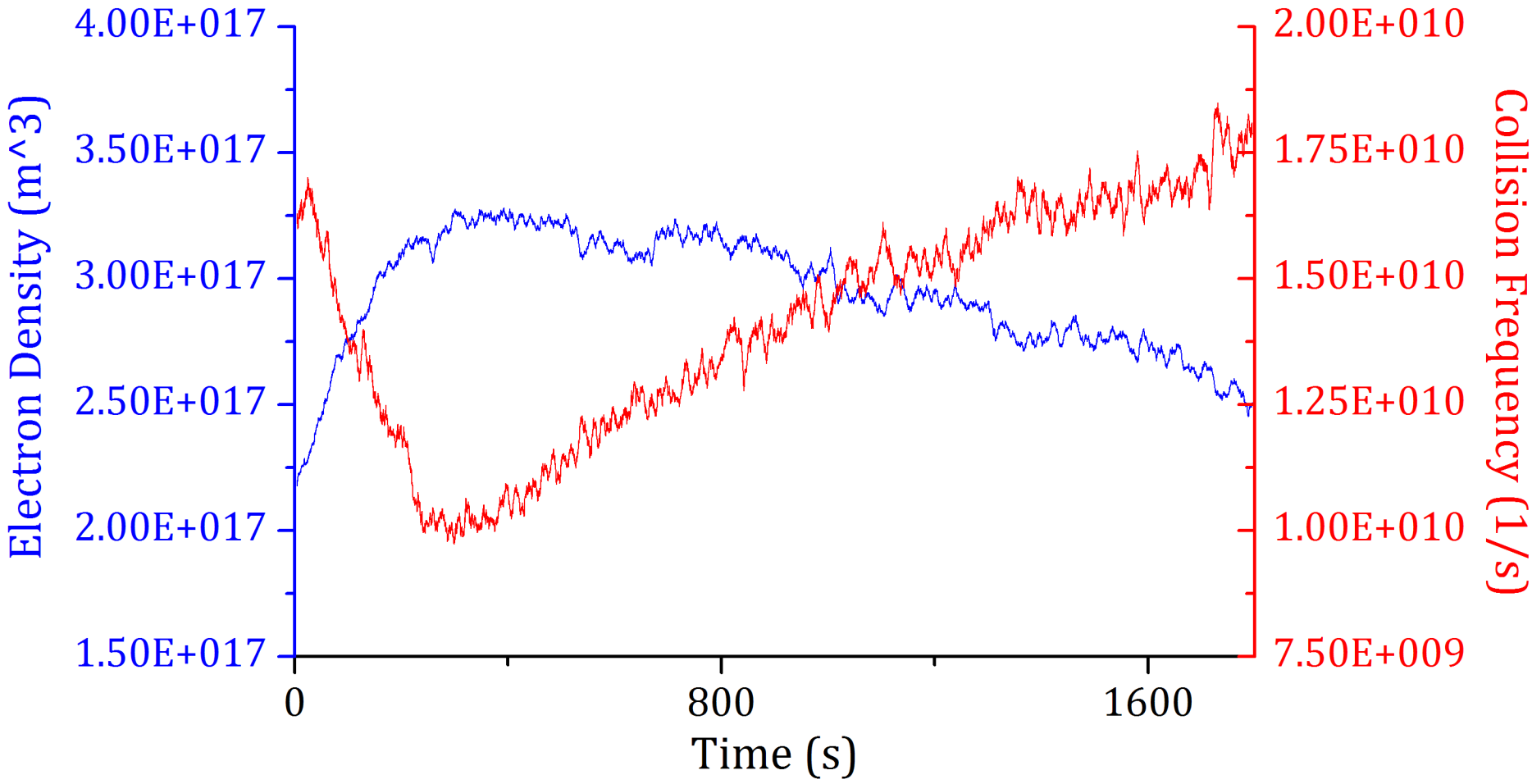

Fig. 8 Measurement of the electron density and collision frequency using mm-wave interferometry. Discharge was operated at 20 kHz with a V_{pp} of 18 kV at 20.9-21.2 Torr.

VII. CARS Spectroscopy

- Target molecule elevated to first vibrational state, $^1\Sigma^+$, by pump, ω_1, and Stokes, ω_2, pulses
  - Probed by additional ω_1 pulse

- Direct transition to ground for diatomic molecules generally forbidden

- Electric field acts as alternate probe in limit of zero frequency allowing emission at ω_{ir}

- Ratio of CARS signal intensity with infrared signal intensity proportional to electric field squared

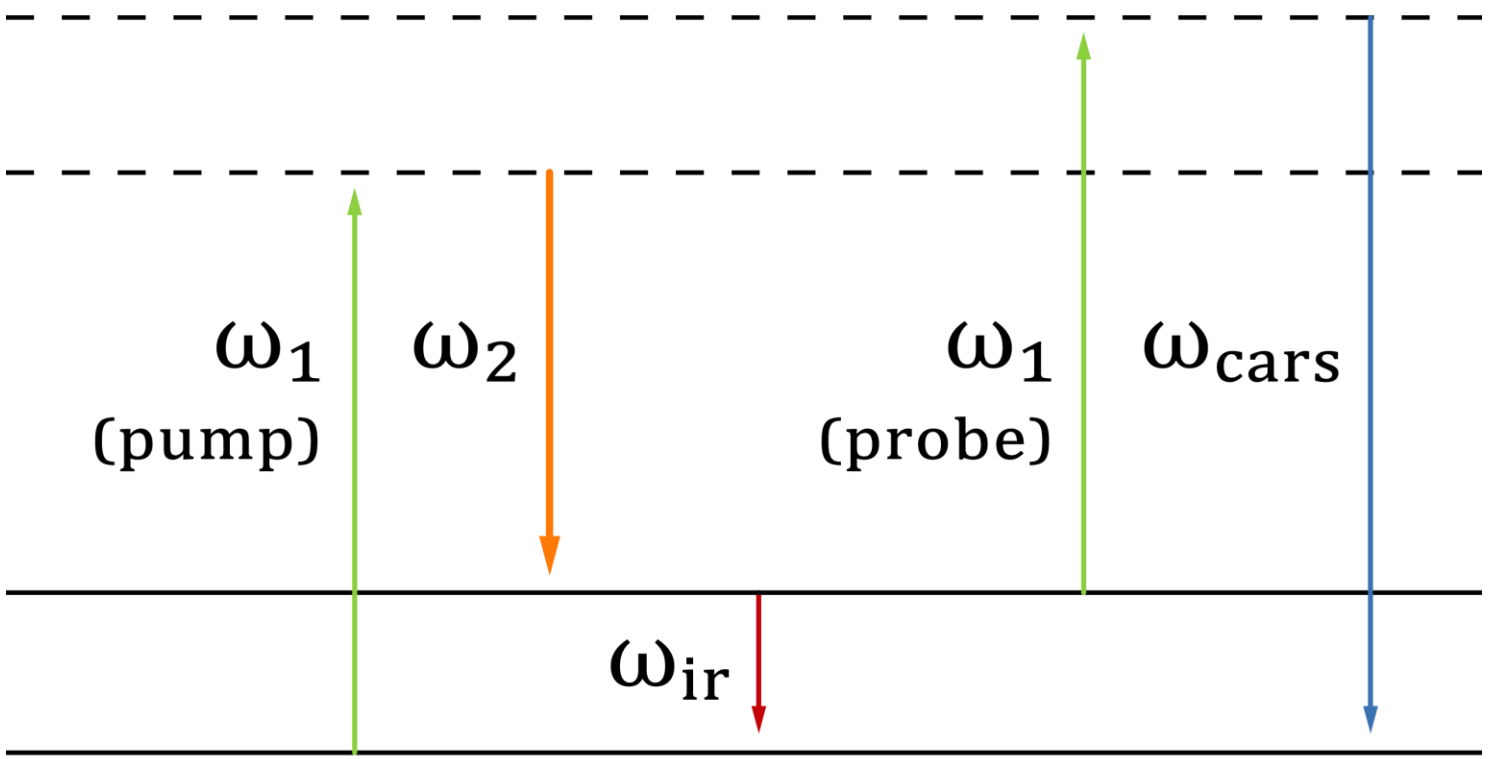

Fig. 3 Diagram of CARS method used to obtain electric field information. The solid lines represent vibrational levels and the dashed lines represent virtual levels.

VIIb. Electric Field Measurements

- Light generated by optical parametric amplifier (OPA), pumped by a Ti:Sapphire laser
- OPA tuned such that signal provides pump/probe and idler provides Stokes pulse
- Light separated by CF_2 and SF11 prisms
- Coherent signals measured by photodiode and InSb detector

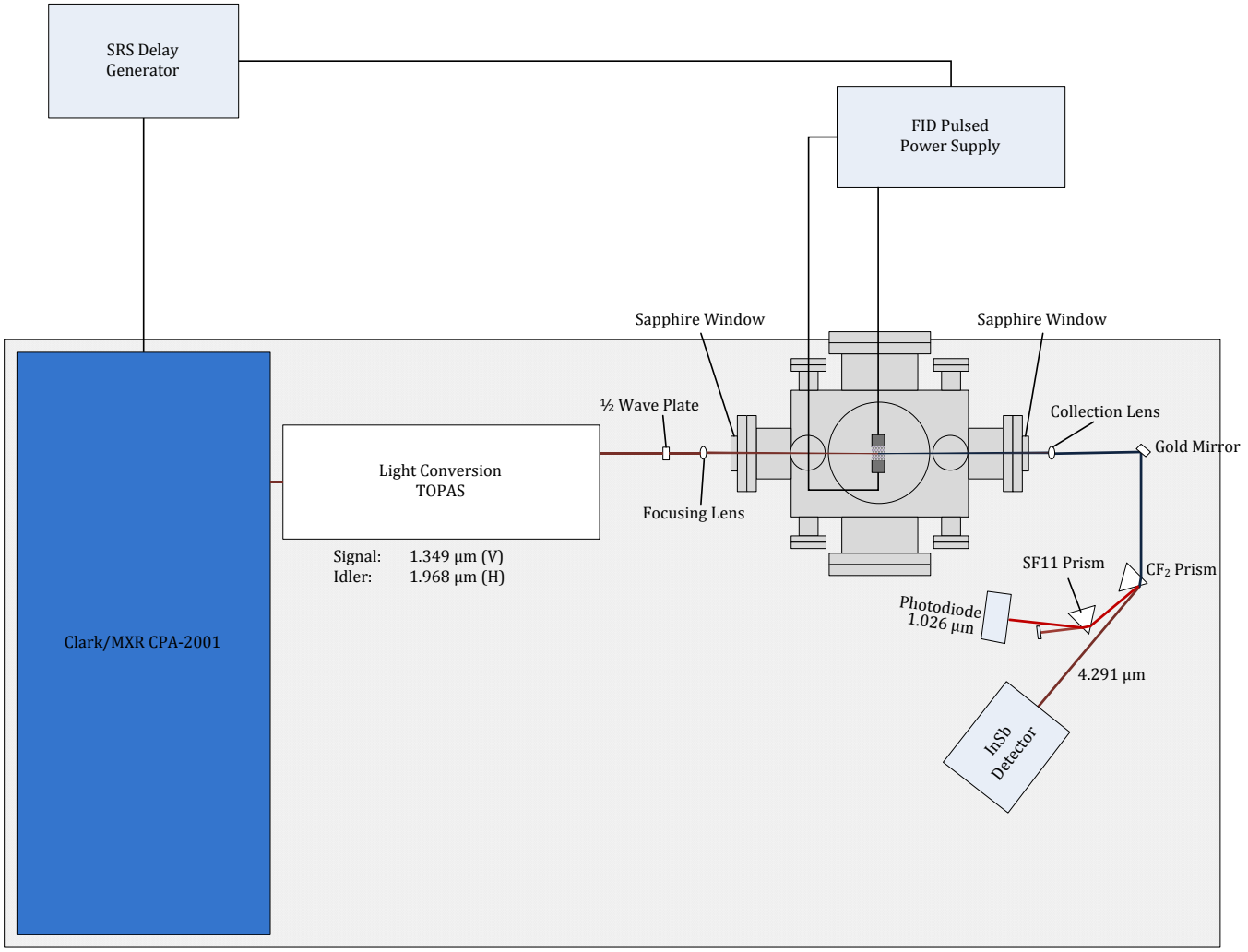

Fig. 9 Sketch of the optical path to be used for the non-intrusive electric field measurement.

Literature Cited:

1. O. A. Evsin, E. B. Kupryanova, V. N. Ochkin, S. Yu Savinov, and S. N. Tskhaĭ, Quant. Elec. 25, 278 (1995).
2. S. J. Schneider, H. Kamhawi and I. M. Blankson, 47th Aerospace Sciences Meeting, Orlando, FL; AIAA: Reston, 2009; 2009-1050.
3. D. S. Nikandrov, L. D. Tsendin, V. I. Kolobov, and R. R. Arslanbekov, IEEE Trans. Plasma Sci. 36, 131 (2008).
4. C. O. Laux, "Radiation and Nonequilibrium Collisional-Radiative Models," von Karman Institute Lecture Series 2002-07, Physico-Chemical Modeling of High Enthalpy and Plasma Flows, eds. D. Fletcher, J.-M. Charbonnier, G.S.R. Sarma, and T. Magin, Rhode-Saint-Genèse, Belgium, 2002.

Acknowledgements: This project is supported by the NASA GSRP Training grant, #NNX-09AK95H.